GEOPHYSICAL RESEARCH LETTERS, VOL. 34, L02306, doi:10.1029/2006GL027081, 2007

Observation of glacial isostatic adjustment in "stable" North America with GPS

Giovanni F. Sella,[1] Seth Stein,[2] Timothy H. Dixon,[3] Michael Craymer,[4] Thomas S. James,[5] Stephane Mazzotti,[5] and Roy K. Dokka[6]

Received 1 June 2006; revised 31 August 2006; accepted 6 September 2006; published 26 January 2007.

[1] Motions of three hundred and sixty Global Positioning System (GPS) sites in Canada and the United States yield a detailed image of the vertical and horizontal velocity fields within the nominally stable interior of the North American plate. By far the strongest signal is the effect of glacial isostatic adjustment (GIA) due to ice mass unloading during deglaciation. Vertical velocities show present-day uplift (~10 mm/yr) near Hudson Bay, the site of thickest ice at the last glacial maximum. The uplift rates generally decrease with distance from Hudson Bay and change to subsidence (1–2 mm/yr) south of the Great Lakes. The "hinge line" separating uplift from subsidence is consistent with data from water level gauges along the Great Lakes, showing uplift along the northern shores and subsidence along the southern ones. Horizontal motions show outward motion from Hudson Bay with complex local variations especially in the far field. Although the vertical motions are generally consistent with the predictions of GIA models, the horizontal data illustrate the need and opportunity to improve the models via more accurate descriptions of the ice load and laterally variable mantle viscosity. **Citation:** Sella, G. F., S. Stein, T. H. Dixon, M. Craymer, T. S. James, S. Mazzotti, and R. K. Dokka (2007), Observation of glacial isostatic adjustment in ''stable'' North America with GPS, *Geophys. Res. Lett.*, *34*, L02306, doi:10.1029/2006GL027081.

1. Introduction

[2] Postglacial rebound or glacial isostatic adjustment (GIA) is the response of the solid Earth to the changing surface load brought about by the waxing and waning of large-scale ice sheets and glaciers. In the past 20,000 years ice melting and associated GIA have caused up to several hundred meters of relative sea-level rise in different parts of North America. Tilting of relic lake shorelines, changes to modern lake levels, and secular changes to surface gravity observations are other manifestations of the land uplift and subsidence brought about by GIA.

[3] GIA provides insight into three major earth processes or structures. First, the delayed response to deglaciation is one of the few ways of constraining the viscosity structure of the mantle, which is crucial for understanding the mantle convection process that gives rise to plate motions and has a profound role in the planet's thermal history [*Peltier*, 1998a; *Schubert et al.*, 2001]. Second, GIA signals can provide a powerful constraint on the distribution and thickness of ice since the last glacial maximum, about 21,000 years ago. Although the general pattern is known from glacial geomorphology, significant questions remain for which GIA can provide important information [*Dyke et al.*, 2002; *Tarasov and Peltier*, 2004; *Peltier*, 2004]. Third, GIA is suspected to be a major cause of deformation within continental plates, and thus a possible cause or trigger of seismicity in eastern North America and other formerly glaciated areas [e.g., *Stein et al.*, 1979, 1989; *James and Bent*, 1994; *Wu and Johnston*, 2000; *Grollimund and Zoback*, 2001; *Mazzotti and Adams*, 2005].

2. Observations

[4] Until recently, present-day observations of GIA were limited in two important ways. First, horizontal motions could not be accurately observed. Second, vertical motions were measured almost exclusively along coasts via sea and lake level changes, which require climatic, hydrographic and tectonic corrections. Regional leveling lines do provide constraints, but their high costs have made them prohibitive and so in North America these are limited especially in the area of largest uplift near Hudson Bay [*Carrera et al.*, 1991]. The advent of space-geodesy, in particular GPS has change the situation because of its lower costs compared to first order level lines and measures 3-dimensional crustal velocities with accuracies of less than a few mm/yr. GIA motions were successfully observed with space geodesy in Scandinavia [e.g., *Milne et al.*, 2001] and have been a target of study across the much larger area affected by GIA in North America (Scandinavia is roughly the size of Hudson Bay). Initial studies used Very Long Baseline Interferometry and Satellite Laser Ranging data, which are very sparse owing to the cost and large installations required. Although the observations were consistent with motions expected from GIA [*James and Lambert*, 1993; *Mitrovica et al.*, 1993; *Argus et al.*, 1999], their utility was limited by their sparse coverage. First-order features of GIA deformation were also confirmed locally by absolute and relative gravity measurements [*Larson and van Dam*, 2000; *Lambert et al.*, 2001; *Pagiatakis and Salib*, 2003] and regional GPS surveys [*Park et al.*, 2002].

[1] National Geodetic Survey, NOAA, Silver Spring, Maryland, USA.
[2] Department of Geological Sciences, Northwestern University, Evanston, Illinois, USA.
[3] Rosenstiel School of Marine and Atmospheric Sciences, University of Miami, Miami, Florida, USA.
[4] Geodetic Survey Division, Natural Resources Canada, Ottawa, Ontario, Canada.
[5] Geological Survey of Canada, Natural Resources Canada, Sidney, British Columbia, Canada.
[6] Center for GeoInformatics and Department of Civil and Environmental Engineering, Louisiana State University, Baton Rouge, Louisiana, USA.

0094-8276/07/2006GL027081$05.00

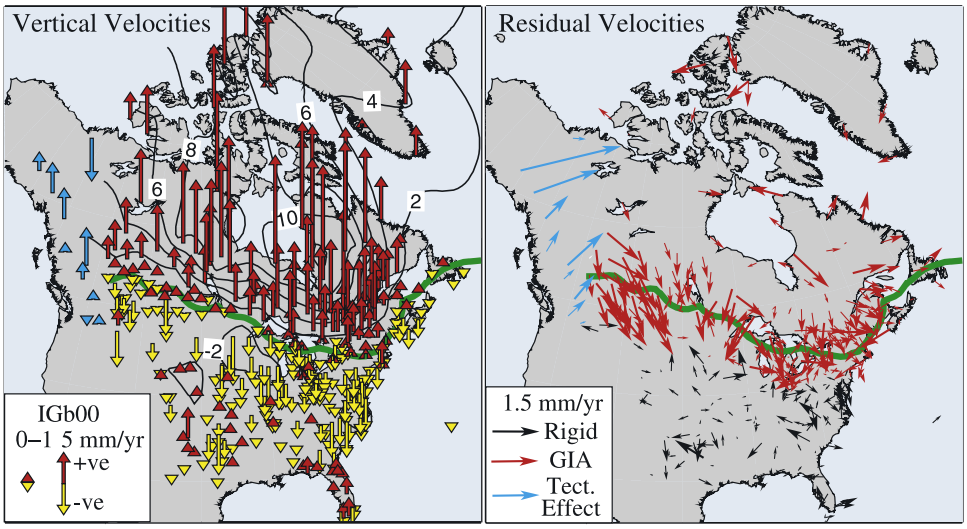

Figure 1. (left) Vertical GPS site motions with respect to IGb00. Note large uplift rates around Hudson Bay, and subsidence to the south. Green line shows interpolated 0 mm/yr vertical "hinge line" separating uplift from subsidence. (right) Horizontal motion site residuals after subtracting best fit rigid plate rotation model defined by sites shown with black arrows. Red vectors represent sites primarily affected by GIA. Purple vectors represent sites that include effects of tectonics.

[5] The density of space geodetic measurements in Eastern North America has recently increased dramatically. Using publicly available continuously recording GPS (CGPS) sites, *Sella et al.* [2002, 2004] identified uplift in areas where significant present-day GIA is expected. Here we use a much larger GPS data set to measure the full three-dimensional surface velocity field. For this purpose, we augment CGPS data with a large set of episodic GPS (EGPS) data collected at sites in Canada that have been occupied for a few days every three to four years. The EGPS data dramatically improve spatial coverage, especially in the critical region of large uplift rates around Hudson Bay near the centre of the former Laurentide ice sheet.

[6] Our data set consists of 362 sites distributed across the interior of North America. Of these, 239 are CGPS sites with time series longer than 3 years (1993–2006), and 123 are EGPS sites with time series longer than 4 years (1994–2005). The EGPS sites are part of the Canadian Base Network, which was created for georeferencing rather than scientific purposes [*Craymer*, 2006]. Nonetheless, these data are of high quality and extraordinarily valuable for GIA studies, as demonstrated along the St. Lawrence Valley [*Mazzotti et al.*, 2005].

[7] All GPS data were processed in the same manner using GIPSY-OASIS software [*Zumberge et al.*, 1997] as described by *Sella et al.* [2002], except that all solutions were aligned with IGb00 [*Ray et al.*, 2004]. Velocities for each site were calculated using a weighted least squares line fit to daily position estimates. Uncertainties were calculated using a velocity error model that accounts for white (uncorrelated), colored (time-correlated), and random walk noise [*Mao et al.*, 1999; *Dixon et al.*, 2000] (See Table S1 in auxiliary material[1]).

[8] Horizontal motions primarily reflect the rotation of the essentially rigid North American plate about its Euler pole. Hence to identify the horizontal intraplate deformation due to GIA and other possible effects, we estimated and removed the predicted rigid plate motion. To do this, we used 233 CGPS sites in the stable interior of North America as defined by standard geologic and seismological criteria: >100 km away from any significant seismicity to avoid any seismic cycle effects, and away from seismogenic faults or active tectonic geomorphic features [e.g., *Crone and Wheeler*, 2000]. We also excluded sites along the Gulf Coast that may be affected by sediment loading, sediment compaction, and slippage along normal faults. A cubic spline was fit to the IGb00 vertical velocities, and we identified the regional zero velocity line (hinge line) (Figure 1, left). We conservatively interpreted that sites north and within ~200 km south of this line may be significantly affected by GIA (sites shown with red arrows in Figure 1, right). We inverted the remaining 124 site velocities (IGb00) (sites shown by black arrows in Figure 1, right) to derive the best-fit angular velocity for the plate (−5.67°N, −84.75°E, 0.196°/Myr, σ_{major} = 0.8°, σ_{minor} = 0.2°, ζ = −4°, σ_{ω} = 0.0019°/Myr). The fit to these horizontal site velocities yields a reduced chi-squared (χ^2_ν) of 1.0, the expected value if our error model is reasonable and the region is in fact rigid within our data uncertainty i.e. less than 1 mm/yr in the horizontal. Including sites that may be significantly affected by GIA gives a larger misfit (χ^2_ν = 1.5), suggesting that we have identified GIA-affected sites on less-rigid parts of the plate.

[9] The resulting residual velocity field (Figures 1, 2) shows both horizontal and vertical intraplate motions. The horizontal residual field may have a small bias because removing the rigid body rotation – primarily resulting from plate motion – may have removed some of the GIA component. However the clear patterns we see in both components are consistent with being caused by GIA. The vertical velocities show fast rebound (~10 mm/yr) near Hudson Bay, the site of thickest ice at the last glacial maximum, which changes to slower subsidence (1–2 mm/yr) south of the

[1]Auxiliary materials is available at ftp://ftp.agu.org/apend/gl/2006gl027081.

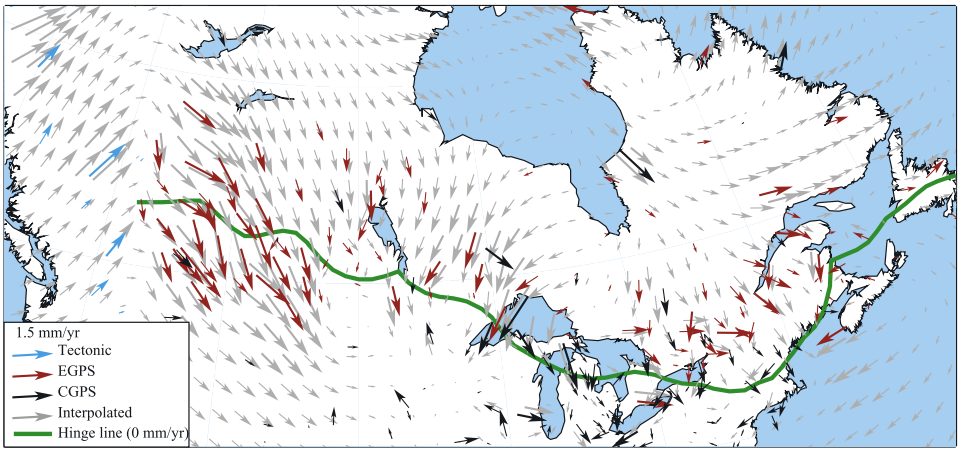

Figure 2. GPS horizontal velocities with motion of rigid North America removed. Interpolated velocity field based on these data derived using GMT software [*Smith and Wessel*, 1990; *Wessel and Smith*, 1998] are shown in light grey.

Great Lakes. This pattern is illustrated by the "hinge line" separating uplift from subsidence, and is consistent with data from water level gauges along the Great Lakes, showing uplift along the northern shores and subsidence along the southern ones [*Mainville and Craymer*, 2005]. On a finer scale, two lobes of high uplift rate east and northwest of Hudson Bay (Figures 1, 3e), appear to correspond with two lobes of maximum ice thickness in a recent ice load model [*Peltier*, 1998a]. However, our data here are quite sparse, and maximum uplift rate need not correlate with maximum ice thickness.

[10] The horizontal velocities are more scattered but show motions directed outward from Hudson Bay and secondary ice maxima in western Canada (Figure 2). In addition, the motions show a pattern of south-southeast-directed flow in southwestern Canada. Some of the horizontal scatter is presumably a combination of local site effects (noise for present purposes) and intraplate tectonic signal, but the pattern beyond the GIA signal is not clear. The results from this very dense field are consistent with other analyses of CGPS sites [*Calais et al.*, 2006] and the Canadian EGPS and CGPS sites [*Henton et al.*, 2006].

3. Model Comparison

[11] The general features of the vertical and horizontal velocity fields are consistent with GIA models (Figures 3 and 4). These models are composed of an ice history (extent and thickness) that loads a specified Earth rheological model. The global ICE-3G model [*Tushingham and Peltier*, 1991] was developed assuming a viscosity structure now termed VM1 that features an upper mantle viscosity of 10^{21} Pa s and lower mantle viscosity twice that. Successors to ICE-3G, ICE- 4G [*Peltier*, 1994] and ICE-5G [*Peltier*, 1998b, 2004] feature revised ice models and are now coupled with a different viscosity structure called VM2 [*Peltier*, 2002]. The viscosity of VM2 varies in a complicated way with depth, but features averaged upper- and lower-mantle viscosities of about 4×10^{20} Pa s and 2×10^{21} Pa s. In other words, VM2 has on average one half the viscosity in the upper mantle as VM1.

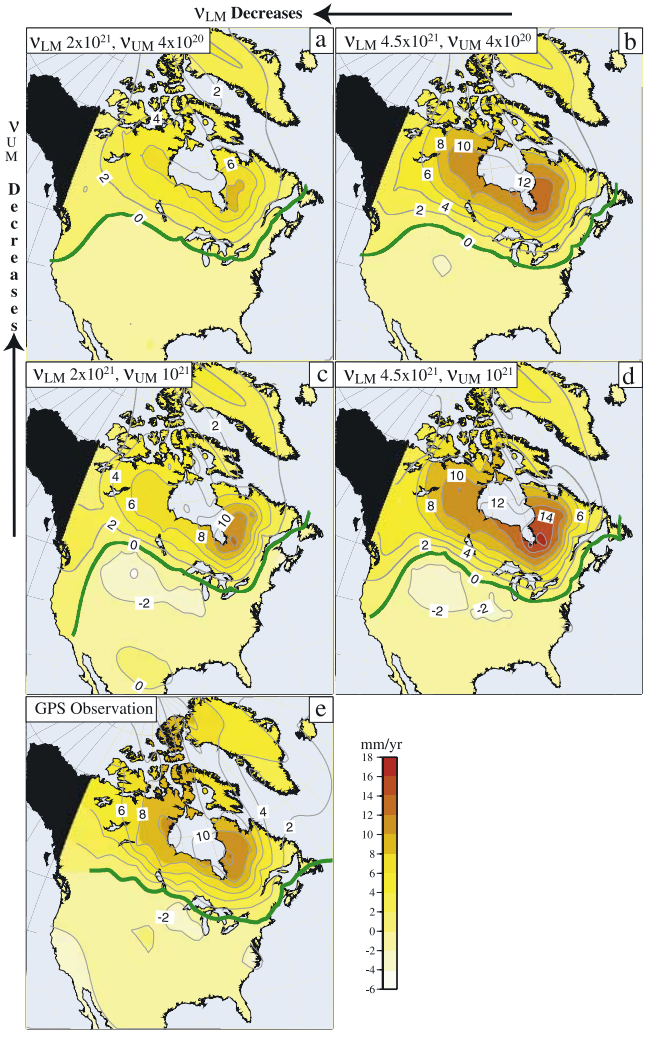

Figure 3. (a–d) Comparison of predicted vertical motion for four different viscosity structures. (e) The predicted motions for each model match the GPS data well. Green line is interpolated hinge line 0 mm/yr.

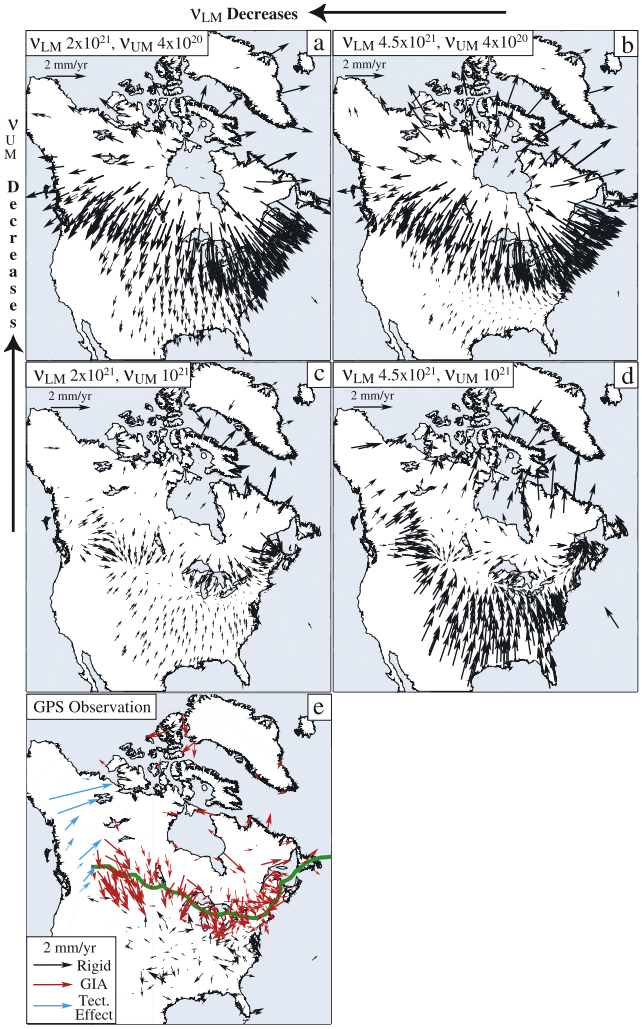

Figure 4. (a–d) Comparison of predicted horizontal motion for four different viscosity structures. (e) The predicted motions differ significantly, and none fit the GPS data well. Green line is interpolated 0 mm/yr vertical hinge line.

[12] The GIA models predict uplift as land under the former ice load rebounds, and subsidence around it as the forebulge beyond the ice sheet margin collapses. Horizontal motion, due primarily to unbending of the lithosphere and asthenospheric relaxation and flow, is minimum under the load center, points outward from the load center at larger distances, and then reverses and points inward. Although the general pattern of upward versus downward motion and toward versus away from the maximum load in Hudson Bay is robust, the predicted magnitude and details of these effects can vary significantly between models. They depend on both the ice loading history and mantle viscosity structure [e.g., *Mitrovica et al.*, 1993; *Peltier*, 1998b; *Milne et al.*, 1999].

[13] We considered four variants of the ICE-3G postglacial rebound model with different upper- and lower-mantle viscosity structures, for a laterally homogeneous Earth model with seismically realistic depth-varying density and elastic parameter profiles. The models feature a 120-km-thick elastic lithosphere and a mantle with a linear Maxwell viscoelastic rheology. ICE-3G describes the history of the major global ice complexes, including the Laurentide ice sheet, from Last Glacial Maximum to the present. For the predictions used here the load is assumed to increase linearly from nil at 100,000 years BP to its maximum at 18,000 years BP, then decrease at 1000-year increments. Ice melting is handled via self-consistent ocean loading.

[14] Comparison of the models in Figures 3 and 4 shows several trends. Lowering the upper mantle viscosity for constant lower mantle viscosity (columns upward) decreases the uplift rate, because more of the relaxation has already occurred. Lowering the lower mantle viscosity for constant upper mantle viscosity (rows leftward) has a similar effect. In addition, the subsidence rate in the forebulge area decreases for lower viscosity values in the upper mantle. Horizontal motions vary even more dramatically. Lowering the upper mantle viscosity (columns upward) broadens the region of outward motion and speeds it up. For the values shown, the broader outward flow region associated with the main ice sheet centered on Hudson Bay overwhelms the effect of the secondary lobe in the Canadian Rockies.

[15] Models with upper mantle viscosity in the range 4×10^{20} to 1×10^{21} Pa s, and lower mantle viscosity in the range 2 to 4.5×10^{21} Pa s, fit the vertical data quite well. However it is not possible to simultaneously fit all the horizontal data with such models; models that fit the near field (near Hudson Bay) data significantly misfit the far field data, and vice versa. For lower mantle viscosities in the range $2.0–4.5 \times 10^{21}$ Pa s, higher upper mantle viscosities (10^{21} Pa s) predict radially inward velocities over a large part of the U.S., whereas a lower viscosity upper mantle (4×10^{20} Pa s) predicts a radially outward pattern.

4. Prospects

[16] These misfits illustrate the potential of GPS data for improving GIA models. The major reasons for model misfit are uncertainties associated with the ice load history, and the assumption of laterally homogeneous rheology. Figure 5 shows the effect of a larger ice load west of Hudson Bay, as now included in the newer ICE-5G model [*Peltier*, 2004]. Although the present data density here is too low to test this difference, additional GPS data could. In addition, lateral variations of both upper mantle viscosity and lithospheric thickness are expected from seismological data [e.g., *Goes and van der Lee*, 2002], and would have a profound impact on the computed surface response to a given ice load history [*Wu and Mazzotti*, 2006]. GIA models developed to explain relative sea level variations on a local scale, such as for Britain [*Lambeck et al.*, 1996], Fennoscandia [*Milne et al.*, 2001], the Barents Sea [*Kaufmann and Wolf*, 1996], and the tectonically active west coast of North America [*Clague and James*, 2002] find substantial differences in inferred mantle viscosity. *Dixon et al.* [2004] note that variations in upper mantle temperature and water content between cratonic and western North America could lead to variations of up to three orders of magnitude in upper mantle viscosity, as well as substantial variations in lithospheric thickness.

[17] GIA models have been computed with lateral variations in both lithospheric thickness and mantle viscosity [*Wu and van der Wal*, 2003; *Latychev et al.*, 2005]. A general feature of such models is that flow tends to be

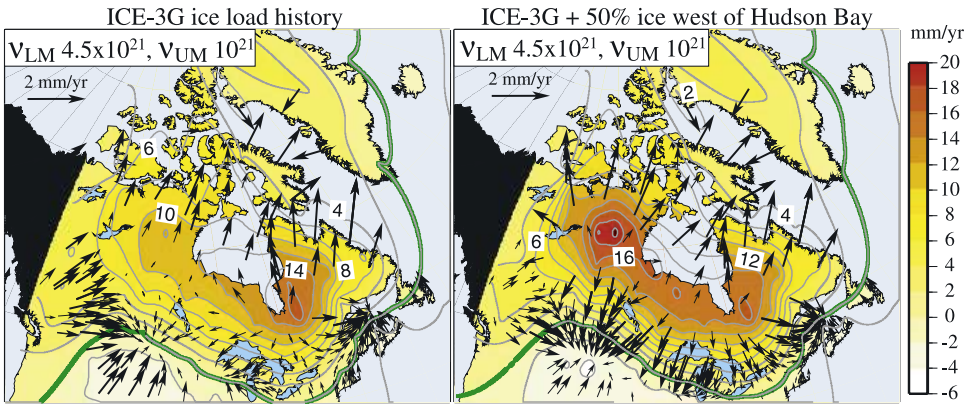

Figure 5. (left) Predicted vertical (color coded contours) and horizontal (arrows) motion for ICE-3G ice load and (right) that load with additional ice west of Hudson Bay. The predicted motions differ significantly and would be resolvable with additional GPS data. Green line is interpolated 0 mm/yr vertical hinge line.

focused toward weaker regions. *Dixon et al.* [2004] describe a large region of low viscosity upper mantle in the western U.S. based on seismic tomography, geodetic data, heat flow, and geochemical indicators of excess water. However the GPS data are not yet sufficiently precise to identify horizontal motion toward this weak zone. An intriguing goal for future studies is to see to what extent, if any, such motion occurs.

[18] **Acknowledgments.** This research was supported by grants EAR-9725585 to T.H.D. and R.K.D. and USGS NEHERP-03HQGR0104 to S.S. We thank two anonymous reviewers for their helpful comments. This is Geological Survey of Canada contribution number 20060415.

References

Argus, D. F., W. R. Peltier, and M. W. Watkins (1999), Glacial isostatic adjustment observed using very long baseline interferometry and satellite laser ranging geodesy, *J. Geophys. Res.*, *104*, 29,077–29,093.

Calais, E., J. Y. Han, C. DeMets, and J. M. Nocquet (2006), Deformation of the North American plate interior from a decade of continuous GPS measurements, *J. Geophys. Res.*, *111*, B06402, doi:10.1029/2005JB004253.

Carrera, G., P. Vanicek, and M. Craymer (1991), The compilation of a map of vertical crustal movements in Canada, *Contract Rep. 91-001*, 100 pp., Geod. Surv. Div., Nat. Resour. Can., Ottawa.

Clague, J. J., and T. S. James (2002), History and isostatic effects of the last ice sheets in southern British Columbia, *Quat. Sci. Rev.*, *21*, 71–87.

Craymer, M. R. (2006), The Evolution of NAD83 in Canada, *Geomatica*, *60*, 151–164.

Crone, A. J., and R. L. Wheeler (2000), Data for Quaternary faults, liquefaction features, and possible tectonic features in the central and eastern United States, east of the Rocky Mountain Front, *U.S. Geol. Surv. Open File Rep. 00-0260*, 342 pp.

Dixon, J., T. H. Dixon, D. R. Bell, and R. Malservisi (2004), Lateral variation in upper mantle viscosity: Role of water, *Earth Planet. Sci. Lett.*, *222*, 451–467.

Dixon, T. H., M. Miller, F. Farina, H. Wang, and D. Johnson (2000), Present-day motion of the Sierra Nevada block and some tectonic implications for the Basin and Range Province, North American Cordillera, *Tectonics*, *19*, 1–24.

Dyke, A. S., J. T. Andrews, P. U. Clark, J. H. England, G. H. Miller, J. Shaw, and J. J. Veillette (2002), The Laurentide and Innuitian ice sheets during the last glacial maximum, *Quat. Sci. Rev.*, *21*, 9–31.

Goes, S., and S. van der Lee (2002), Thermal structure of the North American uppermost mantle inferred from seismic tomography, *J. Geophys. Res.*, *107*(B3), 2050, doi:10.1029/2000JB000049.

Grollimund, B., and M. D. Zoback (2001), Did deglaciation trigger intraplate seismicity in the New Madrid seismic zone?, *Geology*, *29*, 175–178.

Henton, J. A., M. R. Craymer, R. Ferland, H. Dragert, S. Mazzotti, and D. L. Forbes (2006), Crustal motion and deformation monitoring of the Canadian landmass, *Geomatica*, *60*, 173–191.

James, T. S., and A. L. Bent (1994), A comparison of eastern North America seismic strain-rates to glacial rebound strain-rates, *Geophys. Res. Lett.*, *21*, 2127–2130.

James, T. S., and A. Lambert (1993), A comparison of VLBI data in the ICE-3G glacial rebound model, *Geophys. Res. Lett.*, *20*, 871–874.

Kaufmann, G., and D. Wolf (1996), Deglacial land emergence and lateral upper-mantle heterogeneity in the Svalbard Archipelago: II. Extended results for high-resolution load models, *Geophys. J. Int.*, *127*, 125–140.

Lambeck, K., P. Johnston, C. Smither, and M. Nakada (1996), Glacial rebound of the British Isles: III. Constraints on mantle viscosity, *Geophys. J. Int.*, *125*, 340–354.

Lambert, A. N., N. Courtier, G. S. Sasagawa, F. Klopping, D. Winester, T. S. James, and J. O. Liard (2001), New constraints on Laurentide postglacial rebound from absolute gravity measurements, *Geophys. Res. Lett.*, *28*, 109–112.

Larson, K. M., and T. van Dam (2000), Measuring postglacial rebound with GPS and absolute gravity, *Geophys. Res. Lett.*, *27*, 3925–3928.

Latychev, K., J. X. Mitrovica, M. E. Tamisiea, J. Tromp, and R. Moucha (2005), Influence of lithospheric thickness variations on 3-D crustal velocities due to glacial isostatic adjustment, *Geophys. Res. Lett.*, *32*, L01304, doi:10.1029/2004GL021454.

Mainville, A., and M. Craymer (2005), Present-day tilting of the Great Lakes region based on water level gauges, *Geol. Soc. Am. Bull.*, *117*, 1070–1080.

Mao, A., C. Harrison, and T. Dixon (1999), Noise in GPS time series, *J. Geophys. Res.*, *104*, 2797–2816.

Mazzotti, S., and J. Adams (2005), Rates and uncertainties on seismic moment and deformation in eastern Canada, *J. Geophys. Res.*, *110*, B09301, doi:10.1029/2004JB003510.

Mazzotti, S., T. S. James, J. Henton, and J. Adams (2005), GPS crustal strain, postglacial rebound, and seismic hazard in eastern North America: The Saint Lawrence valley example, *J. Geophys. Res.*, *110*, B11301, doi:10.1029/2004JB003590.

Milne, G. A., J. X. Mitrovica, and J. L. Davis (1999), Near-field hydroisostasy: The implications of a revised sea-level equation, *Geophys. J. Int.*, *139*, 464–482.

Milne, G. A., J. L. Davis, J. X. Mitrovica, H. G. Scherneck, J. M. Johansson, M. Vermeer, and H. Koivula (2001), Space-geodetic constraints on glacial isostatic adjustment in Fennoscandia, *Science*, *291*, 2381–2385.

Mitrovica, J. X., J. L. Davis, and I. I. Shapiro (1993), Constraining proposed combinations of ice history and Earth rheology using VLBI determined baseline length rates in North America, *Geophys. Res. Lett.*, *20*, 2387–2390.

Pagiatakis, S. D., and P. Salib (2003), Historical relative gravity observations and the time rate of change of gravity due to postglacial rebound and other tectonic movements in Canada, *J. Geophys. Res.*, *108*(B9), 2406, doi:10.1029/2001JB001676.

Park, K., R. S. Nerem, J. L. Davis, M. S. Schenewerk, G. A. Milne, and J. X. Mitrovica (2002), Investigation of glacial isostatic adjustment in the northeast U.S. using GPS measurements, *Geophys. Res. Lett.*, *29*(11), 1509, doi:10.1029/2001GL013782.

Peltier, W. R. (1994), Ice age paleotopography, *Science*, *265*, 195–201.

Peltier, W. R. (1998a), Postglacial variations in the level of the sea: Implications for climate dynamics and solid-Earth geophysics, *Rev. Geophys.*, *36*, 603–689.

Peltier, W. R. (1998b), A space geodetic target for mantle viscosity discrimination: Horizontal motions induced by glacial isostatic adjustment, *Geophys. Res. Lett.*, *25*, 543–546.

Peltier, W. R. (2002), Global glacial isostatic adjustment: Palaeogeodetic and space-geodetic tests of the ICE-4G (VM2) model, *J. Quat. Sci.*, *17*, 491–510.

Peltier, W. R. (2004), Global glacial isostasy and the surface of the ice-age Earth: The ICE-5G (VM2) model, *Annu. Rev. Earth Planet. Sci.*, *32*, 111–149.

Ray, J., D. Dong, and Z. Altamimi (2004), IGS reference frames, *GPS Solutions*, *8*, 251–266.

Schubert, G., D. Turcotte, and P. Olson (2001), *Mantle Convection in the Earth and Planets*, 940 pp., Cambridge Univ. Press, New York.

Sella, G. F., T. H. Dixon, and A. Mao (2002), REVEL: A model for recent plate velocities from space geodesy, *J. Geophys. Res.*, *107*(B4), 2081, doi:10.1029/2000JB000033.

Sella, G., S. Stein, S. Wdowinski, T. Dixon, and R. Dokka (2004), GPS observation of glacial isostatic adjustment in North America, *Cah. Cent. Eur. Geod. Seismol.*, *23*, 105–110.

Smith, W. H. F., and P. Wessel (1990), Gridding with continuous curvature splines in tension, *Geophysics*, *55*, 293–305.

Stein, S., N. H. Sleep, R. J. Geller, S. C. Wang, and G. C. Kroeger (1979), Earthquakes along the passive margin of eastern Canada, *Geophys. Res. Lett.*, *6*, 537–540.

Stein, S., S. Cloetingh, N. Sleep, and R. Wortel (1989), Passive margin earthquakes, stresses, and rheology, in *Earthquakes at North-Atlantic Passive Margins: Neotectonics and Postglacial Rebound*, edited by S. Gregerson and P. Basham, pp. 231–260, Springer, New York.

Tarasov, L., and W. R. Peltier (2004), A geophysically constrained large ensemble analysis of the deglacial history of the North American ice sheet complex, *Quat. Sci. Rev.*, *23*, 359–388.

Tushingham, A. M., and W. R. Peltier (1991), ICE-3G: A new global model of late Pleistocene deglaciation based upon geophysical predictions of post-glacial relative sea level change, *J. Geophys. Res.*, *96*, 4497–4523.

Wessel, P., and W. H. F. Smith (1998), New, improved version of the Generic Mapping Tools released, *Eos Trans. AGU*, *79*, 579.

Wu, P., and P. Johnston (2000), Can deglaciation trigger earthquakes in North America?, *Geophys. Res. Lett.*, *27*, 1323–1326.

Wu, P., and S. Mazzotti (2006), Effects of a lithospheric weak zone on postglacial seismotectonics in eastern Canada and northeastern USA, in *Continental Intraplate Earthquakes: Science, Hazard, and Policy Issues*, edited by S. Stein and S. Mazzotti, *Geol. Soc. Am. Spec. Pap.*, in press.

Wu, P., and W. van der Wal (2003), Postglacial sealevels on a spherical, self-gravitating viscoelastic earth: Effects of lateral viscosity variations in the upper mantle on the inference of viscosity contrasts in the lower mantle, *Earth Planet. Sci. Lett.*, *211*, 57–68.

Zumberge, J. F., M. B. Heflin, D. C. Jefferson, M. M. Watkins, and F. H. Webb (1997), Precise point positioning for efficient analysis of GPS data, *J. Geophys. Res.*, *102*, 5005–5017.

M. Craymer, Geodetic Survey Division, Natural Resources Canada, Ottawa, ON, Canada, K1A 0E9.

T. H. Dixon, Rosenstiel School of Marine and Atmospheric Sciences, University of Miami, Miami, FL 33149, USA.

R. K. Dokka, Department of Civil and Environmental Engineering, Louisiana State University, Baton Rouge, LA 70803, USA.

T. S. James and S. Mazzotti, Geological Survey of Canada, Natural Resources Canada, Sidney BC, Canada, V8L 4B2.

G. F. Sella, National Geodetic Survey, NOAA, 1315 East-West Highway, Silver Spring, MD 20910, USA. (giovanni.sella@noaa.gov)

S. Stein, Department of Geological Sciences, Northwestern University, Evanston, IL 60208, USA.